Catal Lett (2017) 147:987–995
DOI 10.1007/s10562-016-1940-1

Hydrogenation of 2-Ethylhexenal Using Supported-Metal Catalysts for Production of 2-Ethylhexanol

Guoxiu Liu[1] · Shiwei Liu[1] · Siyuan Liu[1] · Shitao Yu[1] · Lu Li[1] · Fusheng Liu[1] · Congxia Xie[1] · Xiuyan Song[1]

Received: 11 August 2016 / Accepted: 28 November 2016 / Published online: 28 February 2017
© Springer Science+Business Media New York 2016

Abstract The catalytic hydrogenation of 2-ethylhexenal was investigated over Pd supported on ZrO_2, CeO_2, Al_2O_3, MCM-41, MAS-7 and SBA-15. The activities and the selectivities of the catalysts were strongly affected by the nature of the support. Pd/ZrO_2 had an excellent catalytic performance for the hydrogenation. The superior dispersion of Pd on the support ZrO_2, and the stable structure of active components on ZrO_2 as well as the synergistic effect of the bifunctional metal-support interaction enhanced the catalytic performance of Pd/ZrO_2. The conversion of 2-ethylhexenal and the selectivity for 2-ethylhexanol were 100 and 99.1% respectively when the reaction was carried out at 240 °C for 7 h. The product was easily separated from the catalyst and the catalyst was of good reusability when it was repeated six times. In addition, the aggregation of Pd nanoparticles and the coking of ZrO_2 the catalysts were the main cause for the catalyst deactivation.

Graphical Abstract

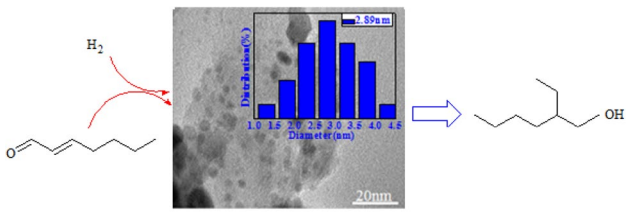

Pd/ZrO_2 catalyst

Keywords Hydrogenation · Catalysis · 2-ethylhexenal · 2-ethylhexanol

1 Introduction

2-Ethylhexanol is an important chemical intermediate and predominately converted to dioctyl adipate and dioctyl phthalate which are excellent and harmless plasticizers for PVC. It is also extensively used in the product of antioxidants, adhesives, cosmetics, surfactants, etc. Currently almost all 2-ethylhexanol starts from the hydroformylation of propene to give *n*-butanal. *N*-Butanal is converted to 2-ethylhexenal by a base catalyzed aldol condensation reaction, and then hydrogenated to obtain 2-ethylhexenol [1]. Among the above process, the hydrogenation of 2-ethylhexenal is a key link in the synthesis of 2-ethylhexenol, and its result directly affects the yield and quality of 2-ethylhexanol. Usually, the hydrogenation is carried out in the gas phase over Ni or Cu catalyst [2–6]. This process has some disadvantages such as high consumption of energy, severe conditions, and low selectivity to the product. Therefore, it is necessary to explore a new approach for the hydrogenation of 2-ethylhexanol.

✉ Shiwei Liu
liushiwei@126.com

✉ Shitao Yu
yushitaoqust@126.com

[1] College of Chemical Engineering and of Chemistry and Molecular Engineering, Qingdao University of Science and Technology, No. 53 Zhengzhou Road, Qingdao 266042, China

The carrier has a great influence on the catalytic performance of the catalyst, and the common catalytic carriers are metal oxide and molecular sieves which generally have high specific surface area and stable structure, and often used to support a variety of metal catalysts such as Pd, Ru, Rh, Ni, Cu and Fe. The obtained supported-metal catalysts can be used for the hydrogenation reaction [7–9], oxidation reaction [10, 11] and condensation reaction [12, 13] with the high conversion of the reagent and selectivity of the desired product. The Ru/C, Ru/SBA, Au/ZrC and Au/ZrO_2 catalysts were used to catalyze the hydrogenation of levulinic acid to γ-valerolactone. Levulinic acid was almost converted to γ-valerolactone with above 90% yield in water solvent, and Au/ZrO_2 showed excellent activity and recyclability which gave 97% yield of γ-valerolactone [14]. The catalyst Ni/Al_2O_3 modified by Cu decreased hydroformylation and methylcyclohexane byproducts by, respectively 70 and 10% the hydrogenation of benzene to cyclohexane [15]. Cu/SBA-15 was an efficient catalyst for the hydrogenation of ethylene carbonate to synthesize ethylene glycol and methanol, and 100% conversion of ethylene carbonate, 94.7% yield of ethylene glycol and 62.3% yield of methanol were achieved [16]. 37% selectivity of γ-butyrolactone was obtained over the Ni/CeO_2 catalyst but only 12.5% selectivity on the Ni/Al_2O_3 for the maleic anhydride hydrogenation [17]. The above results show that the carriers can improve the dispersion of the active ingredient and change the catalytic performance of the catalyst by the interaction with the metal. Although there have been some studies on the hydrogenation of 2-ethylhexenal in the presence of the supported-metal catalyst, they did not achieve the desired catalytic performance. U. Shröder et al. investigated the catalytic performance of Pt/Al_2O_3 on gas-phase hydrogenation of the unsaturated aldehyde with the influence of oxygen, although the addition of oxygen (<0.5%) prevented deactivation on a degree, the side reaction was also carry out and the yield of 2-ethylhexanol was low [18]. A series of supported Ni/γ-Al_2O_3 samples were also prepared and used in the aldehyde hydrogenation, while its excellent activity need relatively high temperature (>400 °C) and the selectivity for 2-ethylhexanol was only 90.5% [19]. Thus, it is necessary to develop an effective hydrogenation catalyst. In this paper, the supported-metal catalysts with different carriers were synthesized and used as catalysts in the hydrogenation of 2-ethylhexenal to produce 2-ethylhexanol. To our surprise, the catalyst Pd/ZrO_2 had an excellent catalytic performance and reusability in the hydrogenation reaction.

2 Experimental

2.1 Materials

Hydrogen (99.9 wt%, Qingdao Tianfu Gas Co. Ltd., China), zirconyl chloride octahydrate (99.9 wt%, Shanghai Macklin Biochemical Co. Ltd., China), cerium (III) nitrate hexahydrate (99.0 wt%, Shanghai Shanfu Chemical Co. Ltd., China), aluminum oxide, MCM-41, SBA-15 and MAS-7 (Suzhou Kangshuo Chemicals Co. Ltd., China), cupric nitrate, zinc nitrate, ammonium dichromate, ruthenium chloride, palladium chloride (99.9 wt%, Wuhan Fengfan Chemicals Co. Ltd., China), and other chemicals (analytical purity) were commercially available. All materials were used without further purification.

2.2 Catalyst Preparation

The supported-metal catalysts were prepared by the deposition-precipitation method, and the detailed process for the synthesis of Pd/ZrO_2 was presented as follows: ZrO_2 carrier was prepared by a coprecipitation method. For a typical synthesis process, the dilute $NH_3{\cdot}H_2O$ solution (0.5 mol/L) was added dropwise into 100 mL 0.2 mol/L $ZrOCl_2{\cdot}8H_2O$ aqueous solution until the pH value of the mixed solution reached 10 at 40 °C obtaining the mother liquid. Then the resultant precipitate was aged in the mother liquid for 12 h, followed by filtration and washing with deionized water and ethanol repeatedly to neutral. The obtained filter cake was dried at 105 °C for 6 h, and then calcined at 500 °C for 4 h in air, giving ZrO_2 powder. Pd/$ZrO_2$was prepared by the deposition-precipitation method. 2.0 g ZrO_2 powder was dispersed in 37.7 mL 0.005 mol/L $PdCl_2$ aqueous solution. 0.5 mol/L Na_2CO_3 aqueous solution was added into until the pH of the dispersion reached 10.5, and then the dispersion was aged at 60 °C for 1 h under stirring which made palladium hydroxide precipitate exclusively on the surface of the ZrO_2 carrier. The resulting solid was separated and washed with distilled water several times to neutral, dried for 6 h at 60 °C and finally calcined at 300 °C in air for 4 h, obtaining the catalyst Pd/ZrO_2 containing about 1.0 wt% Pd [20, 21]. The CeO_2 carrier was prepared in the similar way, and the catalysts Pd/CeO_2, Pd/MCM-41, Pd/MAS-7, Pd/Al_2O_3, Pd/SBA-15 and Pd/C were prepared by the similar deposition-precipitation method. The catalysts Ni/ZrO_2, Co/ZrO_2, Rh/ZrO_2 and Ru/ZrO_2 were also synthesized by the deposition-precipitation method. It was noteworthy that the catalysts Ni/ZrO_2 and Co/ZrO_2 were reduced in a 10% H_2 in N_2 mixture at a heating rate of 5 °C /min and dwelled at 300 °C for 4 h. The Cu/Zn catalyst was prepared by the coprecipitation method. 100 mL 0.5 mol/L $Zn(NO_3)_2$ solution and 100 mL 0.5 mol/L $Cu(NO_3)_2$ solution were mixed. 1.0 mol/L $(NH_4)_2CO_3$ aqueous solution was added

dropwise into the obtained mixture under vigorous stirring until the pH of the reaction mixture was 10. The resulting solution was aged at 30 °C for 3 h. The obtained precipitate was separated, washed 3 times with the distilled water, and dried at 105 °C, then calcined at 400 °C in air, achieving the Cu/Zn catalyst. The Cu/Cr was prepared in the similar way.

The powder X-ray diffraction (XRD) patterns were measured in the range from 5° to 75° using a Rigaku D/max-RA powder diffractometer (Rigaku, Tokyo, Japan) with Cu K radiation (λ = 0.15418 nm). The Brunauer–Emmer–Teller (BET) surface areas of the samples were determined using the nitrogen adsorption method on a Micromeritics ASAP 2020 (Micromeritics Instrument Co., Norcross, GA) at −196 °C. The sample was degassed under vacuum at 200 °C for 4 h prior to adsorption analysis. The high resolution transmission electron microscopy (HR–TEM) measurements were performed using a high resolution TEM JEOL 2100F at 200 keV. Temperature-programmed reduction (H_2-TPR) experiments were carried out in a conventional system equipped with a thermal conductivity detector (TCD). All the samples (100 mg) were pretreated in a quartz U-tube in a flow of pure N_2 at 400 °C for 45 min, then cooled. The reduction reaction was carried out in a flow of 5% H_2 in N_2 from 50 to 900 °C with a linear heating rate of 8 °C/min. The metal contents in the samples were analyzed using a PerkinElmer Optima 5300 DV (PerkinElmer, USA) inductively coupled plasma atomic emission spectrometer (ICP-AES) system with a radio frequency power of 1300 W.

2.3 Hydrogenation of 2–ethylhexenal

2.0 g 2-Ethylhexenal and 0.1 g Pd/ZrO_2 were reacted in a 75 mL stainless-steel autoclave with 6 MPa H_2 at 240 °C for 7 h with stirring agitation (500 r/min), and then the reacted mixture was cooled to room temperature and depressurized. The gas phase material was collected in the air bag, and the upper product was separated by decantation from the catalyst layer. The catalyst layer was reused directly in the recycle experiments. The gas phase material and the liquid phase products were characterized qualitatively with HP6890/5973 GC/MS equipped with an HP5–MS column, 30 m × 0.25 mm × 0.25 μm. No small molecule cracking products were found in the gas phase. The products of 2-ethylhexanol, 2-ethylhexanal and isooctane were detected in the liquid phase. The quantitative analysis of products were determined by GC using HP6890 GC equipped with an HP5–MS column, 30 m × 0.25 mm × 0.25 μm, the contents of the reactants and products were showed by the system of GC chemstation according to the area of each chromatograph peak. The 2-ethylhexenal conversion was defined as *C*%, which is the wt% of 2-ethylhexenal consumed in the reaction. The 2-ethylhexanol (S_{OL}%) selectivity was calculated by: $S_{OL}\% = W_{OL}/W_{ALL} \times 100$, and the 2-ethylhexanal (S_{AL}%) selectivity was calculated by: $S_{AL}\% = W_{AL}/W_{ALL} \times 100$, where W_{OL} and W_{AL} are the amount of 2-ethylhexanol and 2-ethylhexanal, and W_{ALL} is the total amount of the products, including 2-ethylhexanol, 2-ethylhexanal and isooctane, the selectivity of isooctane is lower than 0.1% in all experiments. All experiments were repeated four times in order to determine the reproducibility of the results. The reaction formula is showed in Scheme 1.

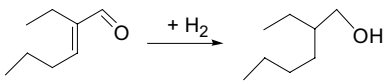

Scheme 1 Hydrogenation of 2-ethylhexenal

Table 1 Effect of catalysts on the hydrogenation

Entry	Catalysts	*C*/%	S_{OL}/%	S_{AL}/%
1	Cu/Cr(1:1)	90.4	92.6	7.4
2	Cu/Zn(1:1)	88.9	90.1	9.9
3	$PdCl_2$(0.02 g)	80.3	88.6	11.4
4	Pd/C	82.5	84.8	15.2
5	Pd/ZrO_2	100	99.1	0.9
6	Pd/Al_2O_3	93.9	89.2	10.8
7	Pd/CeO_2	93.1	95.8	4.2
8	Pd/MAS-7	100	95.6	4.4
9	Pd/MCM-41	96.5	95.1	4.9
10	Pd/SBA-15	95.5	91.3	8.7
11	ZrO_2	/	/	/
12	Rh/ZrO_2	97.6	94.7	5.3
13	Ni/ZrO_2	95.8	89.8	10.2
14	Co/ZrO_2	96.0	90.7	9.3
15	Ru/ZrO_2	97.5	94.9	5.1

2-Ethylhexenal 2.0 g, catalysts 0.10 g, $T = 240$ °C, $t = 7$ h, hydrogen pressure (*P*) 6 MPa. S_{OL} The selectivity of 2-ethylhexanol, S_{AL} The selectivity of 2-ethylhexanal

3 Results and Discussion

3.1 Effects of the Different Catalysts on the Hydrogenation

As can be seen from Table 1, compared with traditional catalysts (Entry 1, 2), the supported-metal catalysts exhibited better catalytic performances. When Cu/Zn or Cu/Cr was used as the catalyst, the utilization rate of 2-ethylhexenal was generally low and 2-ethylhexanal was easily generated, which means that the hydrogenation was not completely carried out. Otherwise, the hydrogenation results were poor

when $PdCl_2$ or Pd/C was used as catalyst (Entry 3 and 4). It is suggested that the above catalysts have the poor catalytic performance for the hydrogenation of 2-ethylhexenal. The different carriers had a significant influence on the catalytic performance of Pd (Entry 5–10). Pd/ZrO_2 showed the best catalytic performance for the hydrogenation with 100% conversion of 2-ethylhexenal and more than 99% selectivity for the desired product 2-ethylhexanol (Entry 5). The results of the catalytic systems, such as Pd/Al_2O_3 and Pd/CeO_2, were not satisfied, though the carriers of the catalytic active component Pd were metal oxides (Entries 6 and 7). Otherwise, the catalytic performance of Pd catalyst system supported by molecular sieve was also poor (Entries 8–10). This may be because of superior dispersion of Pd on the support ZrO_2, the redox surface property of ZrO_2 and the synergistic effect of the bifunctional metal-support interaction [22, 23]. The redox surface property of ZrO_2 improves the transfer of electrons, which also promotes the hydrogenation reaction and the formation of the product [22]. On the other hand, the surface atoms of the monoclinic ZrO_2 have the good structure matching adaptability, and can well match with the catalytic active species such as Pd, PdO and PdO_2. So the carrier ZrO_2 controls the aggregation morphology of the catalytic active species on the surface, which promotes the dispersion of Pd component on the surface of the unit carrier. In order further illustrate the best dispersion of Pd on the carrier ZrO_2, the Pd/ZrO_2 (a), Pd/SBA-15 (b), Pd/Al_2O_3 (c), Pd/MCM-41 (d), Pd/MAS-7 (e) and Pd/CeO_2 (f) were characterized by TEM, and the average particle sizes of Pd on the different supports were quantified. As can been seen from Fig. 1, the average particle sizes of Pd on the support ZrO_2 is 2.89 nm, while the others on the ZrO_2 are more than 3.00 nm, which indicates that the ZrO_2 support has an excellent dispersion performance for Pd nanoparticles. So the catalytic performance of Pd/ZrO_2 was excellent.

When the hydrogenation of the 2-ethylhexenal reaction was performed over the support ZrO_2, it did not exhibit any activity (Entry 11). Therefore, the result also certified the synergistic catalytic performance of Pd and ZrO_2. In order to further illustrate the synergistic effect of the bifunctional metal-support interaction, the samples of ZrO_2 (a), unused Pd/ZrO_2 (b), and repeatedly used eight times Pd/ZrO_2 (c) were analyzed by the XRD, and the results are showed in Fig. 2. As can be seen from Fig. 2a, b, the diffraction peaks with 2θ at 30.3°, 35.2°, 50.2° and 60.2° were observed, which indicates that the ZrO_2 and the unused Pd/ZrO_2 show mainly a tetragonal phase. The diffraction peaks of

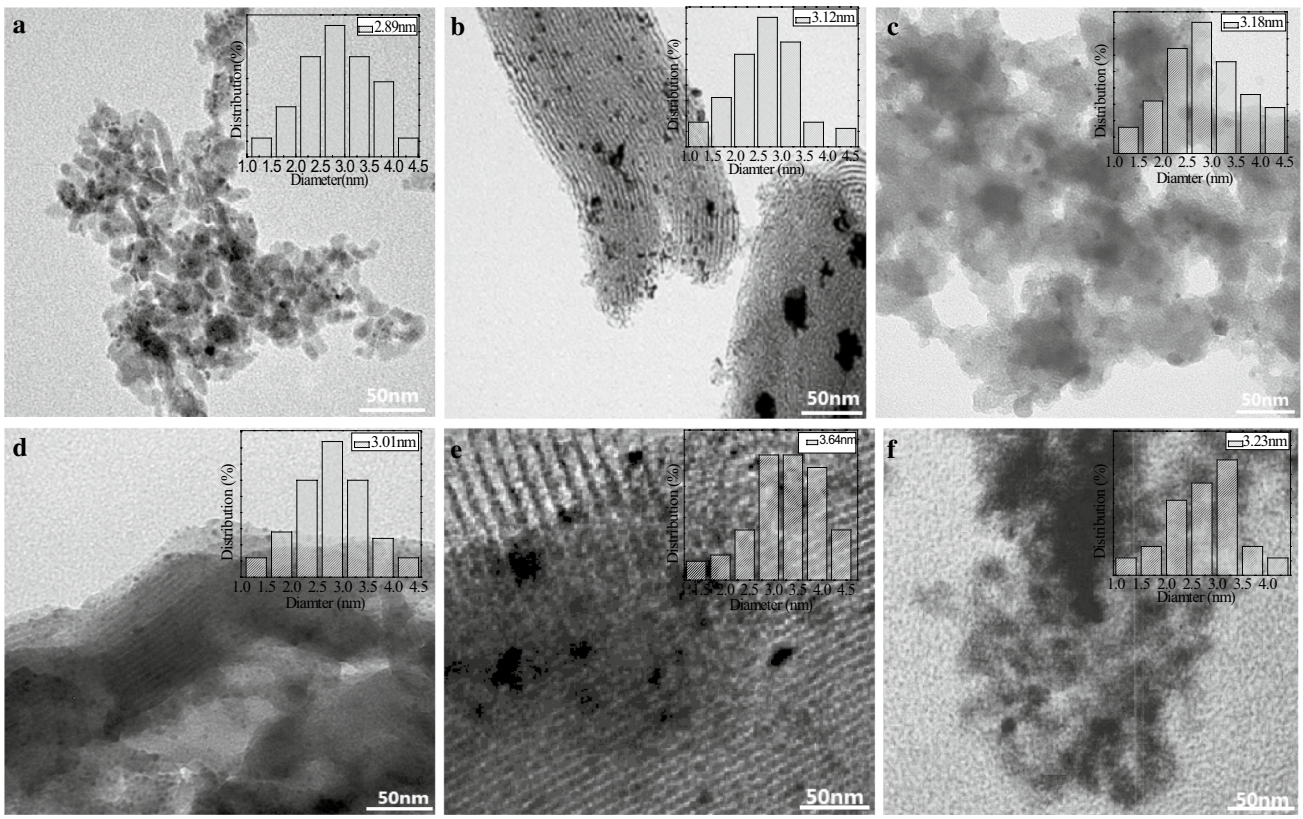

Fig. 1 The TEM images of Pd/ZrO_2 (**a**), Pd/SBA-15 (**b**), Pd/Al_2O_3 (**c**), Pd/MCM-41 (**d**), Pd/MAS-7 (**e**), Pd/CeO_2 (**f**)

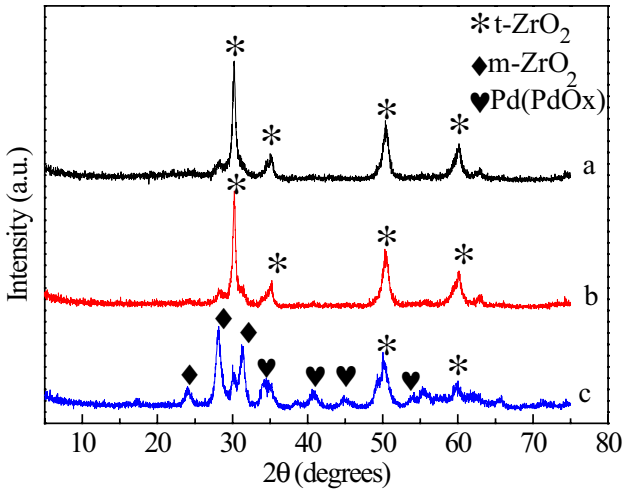

Fig. 2 X-ray diffraction patterns of ZrO_2 (**a**), unused Pd/ZrO_2 (**b**) and repeatedly used eight times Pd/ZrO_2 (**c**)

the unused Pd/ZrO_2were sharper than those of ZrO_2, indicating that palladium oxide is stabilized by the ZrO_2 carrier. No distinct diffraction peak of Pd ($2\theta = 40.5°$), PdO ($2\theta = 34.0°$) and PdO_2 ($2\theta = 54.6°$) were observed from Fig. 2b. The results may be due to that the Pd species are highly dispersed on the surface of carrier ZrO_2. While the diffraction peaks of Pd were identified from Fig. 2c, it may be due to the agglomeration of Pd particles during the reaction which makes the metal expose on the surface of ZrO_2. The diffraction peaks with 2θ at 24.4°, 28.1°, 31.4°. 55.5° assigned to monoclinic ZrO_2 phase, which indicates that the aged Pd/ZrO_2 shows mainly a monoclinic phase [24].

Among the catalytic systems using ZrO_2 as the carrier (Entries 5, 12–15), Pd/ZrO_2 exhibited the best catalytic property, and the conversion of 2-ethylhexenal and the selectivity for 2-ethylhexanol were less than 98% and 95%, respectively. It is indicated that Pd/ZrO_2 is an efficient catalytic system for the carbon carbon double bond and aldehyde group [25]. The catalysts of Ni, Co, Ru, Rh supported on ZrO_2 (Entries 12–15) showed relatively high activity. This may be due to that Ni, Co, Ru and Rh are commonly catalytic centers for the hydrogenation with the good catalytic performance. And ZrO_2 can effectively promote the dispersion of metals which makes the catalyst have high activity.

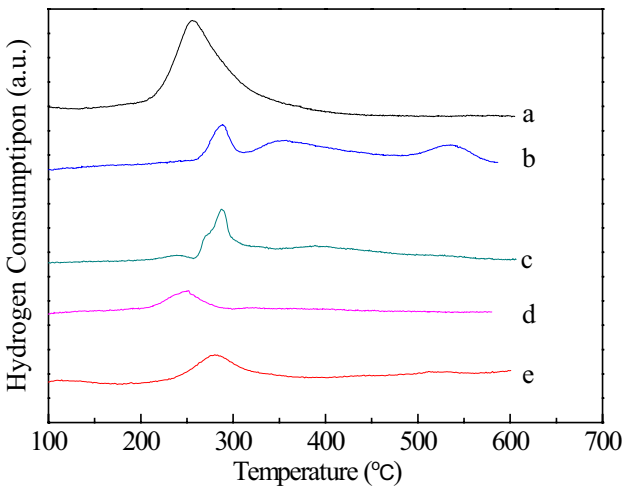

Fig. 3 TPR profiles of Pd/ZrO_2 (*a*), Ni/ZrO_2 (*b*), Co/ZrO_2 (*c*), Rh/ZrO_2 (*d*) and Ru/ZrO_2 (*e*)

To further illustrate the highest activity of Pd/ZrO_2, TPR of the Pd/ZrO_2 (a), Ni/ZrO_2 (b), Co/ZrO_2 (c), Rh/ZrO_2 (d) and Ru/ZrO_2 (e) were characterized and the results are showed in Fig. 3. As can be seen from Fig. 3, the shape of the TPR curve, the size of the peak and the peak top temperature were related to the composition of the catalyst and the nature of the reducible species. In general, with increasing the number of active sites in the catalyst, the initial peak temperature of the reduction peak is lower and the peak area is larger. Compared with the TPR curves of Pd/ZrO_2 (a), Ni/ZrO_2 (b), Co/ZrO_2 (c), Rh/ZrO_2 (d) and Ru/ZrO_2 (e), the peak area of PdO_x/ZrO_2 TPR curve was larger even its reduction temperature was low (240 °C). Otherwise, the contents of the active components were also measured by ICP-AES, and the initial content was almost same for each sample (Pd 0.98 wt%, Ni 0.97 wt %, Co 0.97 wt %, Rh 0.96 wt %, Ru 0.96 wt %).

3.2 Effects of the Reaction Conditions on the Hydrogenation

Figure 4a–d shows the effects of the catalyst dosage, reaction temperature, reaction time and reaction pressure on the hydrogenation using Pd/ZrO_2 as catalyst. It was found that the conversion of 2-ethylhexenal and the selectivity for 2-ethylhexanol increased unpon increasing the catalyst from 0.05 to 0.10 g. So an appropriate increase in the amount of catalyst can effectively improve the hydrogenation. When the catalyst dosage was 0.10 g, the conversion of 2-ethylhexenal and the selectivity for 2-ethylhexanol were 100% and 98.0%, respectively. After that, no significant increase in the 2-ethylhexanol selectivity upon increasing the catalyst dosage could be obtained (Fig. 4a). The reaction temperature had a significant effect on the hydrogenation (Fig. 4b). With decreasing the reaction temperature from 250 to 210 °C, the conversion of 2-ethylhexenal expectedly decreased, while the selectively of 2-ethylhexanol first increased and then decreased, and it was found that some alkane by-product was formed when the reaction temperature was more than 250 °C. It was suggested that too high a temperature enhanced the dehydroxylation of the hydroxyl compound. Therefore, the

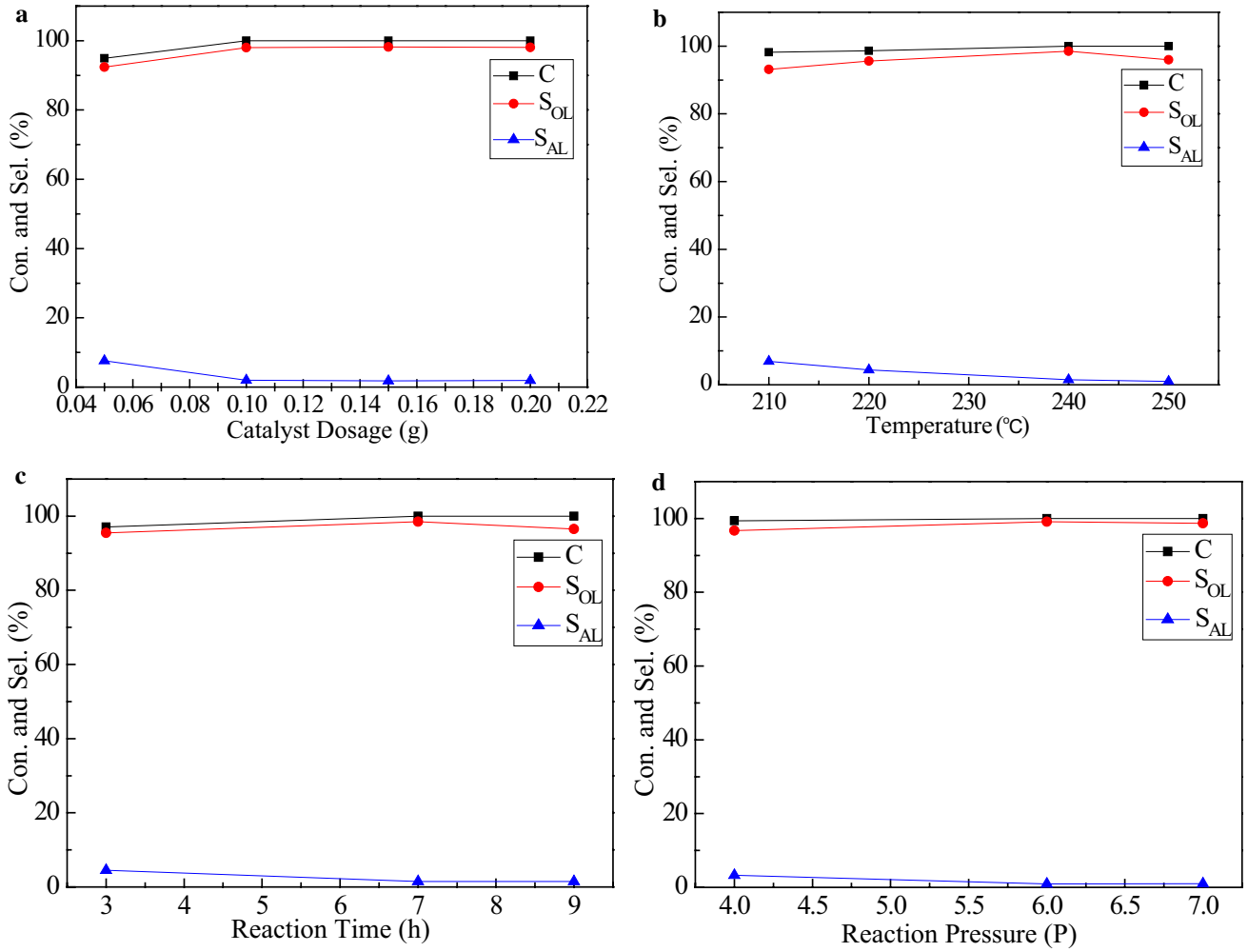

Fig. 4 Effects of catalyst dosage (*a*), reaction temperature (*b*), reaction time (*c*) and reaction pressure (*d*) on the hydrogenation

optimal reaction temperature was 240 °C. The effect of reaction time is also showed in Fig. 4c. With prolonging the reaction time, the conversion of 2-ethylhexenal and the selectivity for 2-ethylhexanol significantly increased. When the reaction time was 7 h, the conversion of 2-ethylhexenal and the selectivity for 2-ethylhexanol were 100 and 98.5%, respectively. However, both did not further change when the time was increased further, and some alkane by-product originating from the dehydroxylation was found when the reaction time was more than 7 h. So the optimal reaction time was 7 h. The H_2 pressure also has an important effect on the hydrogenation (Fig. 4d). With increasing H_2 pressure, the hydrogenation reaction was easy to carry out, and the conversion of 2-ethylhexenal and the selectivity for 2-ethylhexanol were 100 and 99.1% respectively when the reaction was carried out at 240 °C under H_2 pressure 6 MPa. Otherwise the alkane byproduct was not detected. Based on the above results, the optimum reaction conditions were obtained as follows: 2-Ethylhexenal 2.0 g, Pd/ZrO_2 0.10 g, H_2 pressure 6 MPa, reaction temperature 240 °C and reaction time7 h. Under these conditions, the conversion of 2-ethylhexenal

Table 2 Reusability of the catalyst

Times	*C*/%	S_{OL}/%	S_{AL}/%
1	100	98.9	1.1
2	100	98.2	1.8
3	100	98.0	2.0
4	99.8	98.2	1.8
5	99.6	97.5	2.5
6	99.7	97.0	3.0
7	92.6	93.7	6.3
8	86.9	90.1	9.9

2–Ethylhexenal 2.0 g, Pd/ZrO_2 0.10 g, $T = 240$ °C, $t = 7$ h, $P = 6$ MPa.

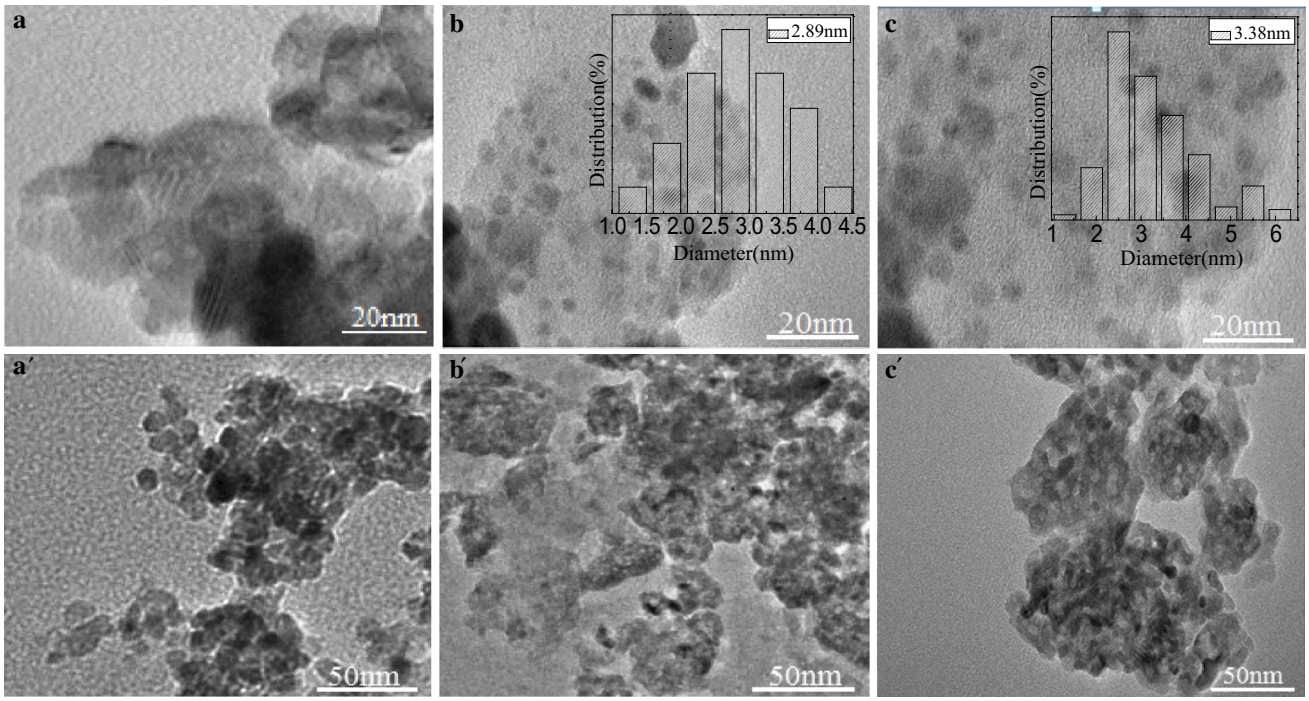

Fig. 5 N_2 adsorption–desorption isotherms of ZrO_2 (*a*), fresh Pd/ZrO_2 (*b*) and aged Pd/ZrO_2 (*c*)

and the selectivity of 2-ethylhexanol were 100 and 99.1%, respectively.

3.3 Reusability of Catalyst

When the reaction was finished, the upper organic phase was separated by centrifugation. Then by adding fresh reagent, Pd/ZrO_2 was directly used to investigate its reusability under the optimum reaction conditions. Results are showed in Table 2. The catalytic system was reused six times without any obvious decrease in the conversion and selectivity, which indicates that the catalyst system is reusable for multiple times. However, the conversion and selectivity slightly decreased for eight times, which may be because of the aggregation of Pd particles and the coking of ZrO_2 during the reaction process. So the preparation and anti-coking capability of carrier is still a lot of work to do. In order to clarify the aggregation of Pd particles and the coking of ZrO_2, BET and TEM analysis were used to test the samples of ZrO_2 (a), unused Pd/ZrO_2 (b), and repeatedly used eight times Pd/ZrO_2 (c), and the results are showed in Fig. 5 and Table 3 and Fig. 6.

Table 3 The characterization results of (ZrO_2 (a), Pd/ZrO_2 (b) and aged Pd/ZrO_2 (c))

Samples	S_{BET} (m^2/g)	Pore volume (cm^3/g)	Pore diameter (nm)
a	68.18	0.24	3.00
b	65.55	0.20	2.96
c	46.20	0.14	1.58

The result of the N_2 adsorption-desorption isotherms is showed in Fig. 5, and the results of the BET surface area, pore volume and pore diameter of catalysts are showed in Table 3. The pore volume and pore size are calculated based on the BJH method. As shown in Fig. 5, the adsorption-desorption isotherms of three samples appear capillary condensation system, which were the typical mesoporous material isotherms, indicating that the mesoporous structure of the repeatedly used eight times Pd/ZrO_2 is not destroyed. As shown in Table 3, the specific surface area of ZrO_2 was 68.18 m^2/g, but that of the unused Pd/ZrO_2 decreased slightly to 65.55 m^2/g. It may be attributed to that the Pd oxides support on the carrier ZrO_2. When Pd/ZrO_2 was repeatedly used eight times, the specific surface area, the pore volume and diameter decreased significantly, which implies that the coking of catalyst blocks the partial pores [26].

The TEM images are showed in Fig. 6. As can be seen from Fig. 6a, a′, b, b′, the particle sizes of ZrO_2 and the unused Pd/ZrO_2 changed slightly, and they were all in nanometer level which indicated that the carrier was stable in the process of catalyst preparation. The images of Fig. 6b, b′ showed that ZrO_2 was spherical or ellipsoidal, and the Pd particles were supported on the ZrO_2 carrier.

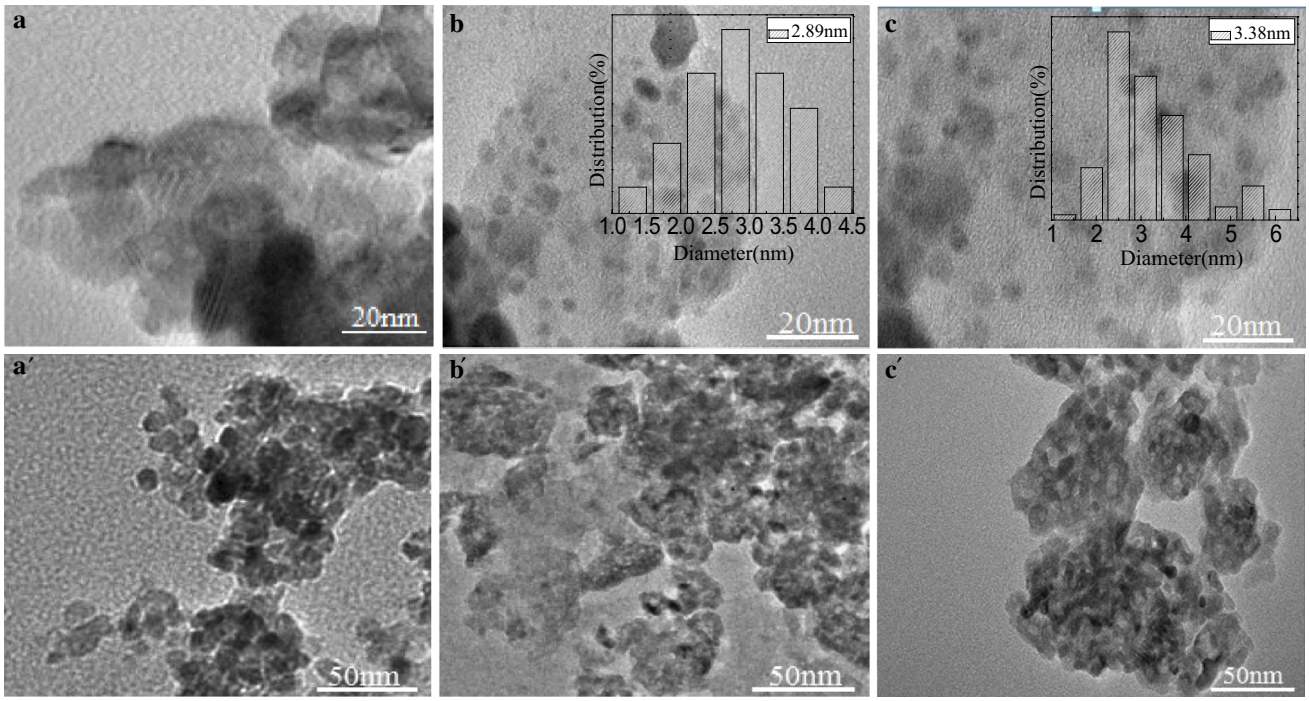

Fig. 6 TEM images of ZrO_2 (**a, a′**), unused Pd/ZrO_2 (**b, b′**) and repeatedly used eight times Pd/ZrO_2 (**c, c′**)

The average particle size of the unused ZrO_2 was 15–25 nm and the average particle size of Pd was 2.89 nm. While the obtained micrographs of the repeatedly used eight times Pd/ZrO_2 revealed that the samples bore agglomerated microstructures, and the result was good agreement with the result of XRD. In particular, the size of the Pd particles was 3.38 nm when Pd/ZrO_2 was repeated used eight times, which was larger than the particle size of the unused Pd/ZrO_2. This phenomenon is mainly ascribed to the aggregation of the Pd particulates.

4 Conclusions

The hydrogenation of 2-ethylhexenal was investigated over Pd supported on ZrO_2, CeO_2, Al_2O_3, MCM-41, MAS-7 and SBA-15. Pd/ZrO_2 had an excellent catalytic performance for the hydrogenation. The superior dispersion of Pd on ZrO_2, the stable structure of active components on ZrO_2 as well as the synergistic effect of the bifunctional metal-support interaction enhanced the catalytic performance of Pd/ZrO_2. 100% conversion of 2-ethylhexenal and 99.1% selectivity for the desired product 2-ethylhexanol were achieved after the reaction was carried out at 240 °C for 7 h. The product was easily separated from the catalyst and the catalyst system was of good reusability when it was repeated six times. In addition, the aggregation of Pd particles and the coking of ZrO_2 the catalysts were the main cause for the deactivation of the catalyst.

Acknowledgements This work was financially supported by the National Basic Research Program of China (973 Program) (2014CB460610), the National Natural Science Foundation of China (No. 30571463) and the TaiShan Scholars Projects of Shandong (No. ts201511033). The authors are grateful for the financial support.

References

1. Hamilton CA, Jackson SD, Kelly GJ (2004) Appl Catal A 263:63
2. Gurevich GS (1987) Khim Prom 10:581.
3. Ludwig GH (1993) Hydrocarb Process 72:67.
4. Niklasson C, Smedler G (1987) Ind Eng Chem Res 26:403
5. Wang XQ, Saleh RY, Ozkan US (2005) J Catal 231:20.
6. Wang XQ, Ozkan US (2005) J Mol Catal A 232:101.
7. Dong XS, Li F, Zhao N, Xiao FK, Wang JW, Tan YS (2016) Appl Catal B 191:8
8. Yan XH, Zhang Q, Zhu MQ, Wang ZB (2016) J Mol Catal A 413:85.
9. Hu CQ, Creaser D, Gronbeck H, Ojagh H, Skoglundh M (2015) Catal Sci Technol 5:1716.
10. Davis SE, Ide MS, Davis RJ (2013) Green Chem 15:17.
11. Santra C, Auroux A, Chowdhury B (2016) RSC Adv 6:45330.
12. Shen WQ, Tompsett GA, Hammond KD, Xing R, Dogan F, Grey CP, Auerbach SM, Huber GW (2011) Appl Catal A 392:57
13. Liang DC, Li GZ, Liu YH, Wu JM, Zhang XW (2016) Catal Commun 81:33
14. Son PA, Nishimura S, Ebitani K (2014) RSC Adv 4:10525.
15. Michalsk K, Kowalik P, Konkol M, Prochniak W, Stołecki K, Słowik G, Borowiecki T (2016) Appl Catal A 523:54

16. Li FJ, Wang LG, Han X, He P, Cao Y, Li HQ (2016) RSC Adv 6:45894.
17. Liao X, Zhang Y, Hill M, Xia X, Zhao YX, Jiang Z (2014) Appl Catal A 488:56
18. Shröder U, Andersson B (1991) J Catal 132:402.
19. Yang R, Li X, Wu J, Zhang X, Zhang Z, Cheng Y, Guo J (2009) Appl Catal A 368:105
20. Wang QC, Liu ZP, An SL, Wang RF, Wang YL, Xu T (2016) J Rare Earth 34:276.
21. Shen WJ, Okumura M, Matsumura Y, Haruta M (2001) Appl Catal A 213:225
22. Han Y, Zhu J (2013) Top Catal 56:1525
23. Souza PMD, Rabelo-Neto RC, Borges LEP, Jacobs G, Davis BH, Graham UM, Resasco DE, Noronha FB (2015) ACS Catal 5:7385.
24. Xu XX, Wang X (2009) Nano Res 2:891
25. Szollosi G, Mastalir A, MolnAr A, Bartok M (1996) React Kinet Catal Lett 57:29
26. Zheng T, He J, Xia W, Hochstadt H, Yang J, Zhao Y (2015) Catal Commun 71:51